CrossMark

CAMBRIDGE
UNIVERSITY PRESS

Research Paper

A SETI survey of the Vela region using the Murchison Widefield Array: Orders of magnitude expansion in search space

C. D. Tremblay[1] and S. J. Tingay[2]

[1]CSIRO Astronomy and Space Science, PO Box 1130, Bentley WA 6102, Australia and [2]International Centre for Radio Astronomy Research, Curtin University, Bentley, WA 6102, Australia

Abstract

Following the results of our previous low-frequency searches for extraterrestrial intelligence (SETI) using the Murchison Widefield Array (MWA), directed towards the Galactic Centre and the Orion Molecular Cloud (Galactic Anticentre), we report a new large-scale survey towards the Vela region with the lowest upper limits thus far obtained with the MWA. Using the MWA in the frequency range 98–128 MHz over a 17-h period, a 400 $\deg^2$ field centred on the Vela Supernova Remnant was observed with a frequency resolution of 10 kHz. Within this field, there are six known exoplanets. At the positions of these exoplanets, we searched for narrow-band signals consistent with radio transmissions from intelligent civilisations. No unknown signals were found with a 5σ detection threshold. In total, across this work plus our two previous surveys, we have now examined 75 known exoplanets at low frequencies. In addition to the known exoplanets, we have included in our analysis the calculation of the Effective Isotropic Radiated Power (EIRP) upper limits towards over 10 million stellar sources in the Vela field with known distances from *Gaia* (assuming a 10-kHz transmission bandwidth). Using the methods of Wright, Kanodia, & Lubar (2018) to describe an eight-dimensional parameter space for SETI searches, our survey achieves the largest search fraction yet, two orders of magnitude higher than the previous highest (our MWA Galactic Anticentre survey), reaching a search fraction of $\sim 2 \times 10^{-16}$. We also compare our results to previous SETI programs in the context of the $\mathrm{EIRP_{min}}$—Transmitter Rate plane. Our results clearly continue to demonstrate that SETI has a long way to go. But, encouragingly, the MWA SETI surveys also demonstrate that large-scale SETI surveys, in particular for telescopes with a large field-of-view, can be performed commensally with observations designed primarily for astrophysical purposes.

Keywords: planets and satellites: detection – radio lines: planetary systems – instrumentation: interferometers – techniques: spectroscopic

(Received 27 May 2020; revised 24 July 2020; accepted 27 July 2020)

1. Introduction

In this paper, we continue to report on our program to utilise the Murchison Widefield Array (MWA: Tingay et al. 2013; Wayth et al. 2018) in a Search for Extraterrestrial Intelligence (SETI) at low radio frequencies, over extremely wide fields of view.

In previous work, we have examined two survey fields, encompassing 400 $\deg^2$ towards the Galactic Centre in the frequency range 103–133 MHz (Tingay et al. 2016) and 625 $\deg^2$ towards the Galactic Anticentre direction in the frequency range of 99–122 MHz (Tingay, Tremblay, & Croft 2018). In these two survey fields, 45 and 22 exoplanets were known at the times of observation, respectively, and no candidate signals were detected above the observational detection limits, which were approximately 4×10^{13} and 1×10^{13} W for the closest exoplanets in the fields, respectively (assuming isotropic transmitters and a 10-kHz transmission bandwidth to calculate Effective Isotropic Radiated Power (EIRP)).

Author for correspondence: C. D. Tremblay, E-mail: chenoa.tremblay@csiro.au
Cite this article: Tremblay CD and Tingay SJ. (2020) A SETI survey of the Vela region using the Murchison Widefield Array: Orders of magnitude expansion in search space. *Publications of the Astronomical Society of Australia* **37**, e035, 1–7. https://doi.org/10.1017/pasa.2020.27

A general improvement in our data processing techniques between the two sets of observations, and the fact that on average the known exoplanets towards the Galactic Anticentre are closer than those known towards the Galactic Centre, means that our upper limits on the EIRP for exoplanets towards the Galactic Anticentre are lower, in general. Tingay et al. (2018) placed our results to that point in the context of the overall SETI endeavour and we refer the reader to that discussion and references therein for this context.

The MWA provides a unique facility to search for technosignatures at low radio frequencies, being highly sensitive, located at the radio-quiet Murchison Radio-astronomy Observatory (MRO), and having a very wide field-of-view (the surveyed areas noted above represent single MWA pointings). The Galactic Centre field survey we previously reported was placed in the context of past SETI surveys by Gray & Mooley (2017), who show that the limits we achieved are highly competitive. In their analysis of 'How Much SETI Has Been Done? Finding Needles in the n-dimensional Cosmic Haystack', Wright et al. (2018) examine an eight-dimensional parameter space for radio SETI and find our two previous surveys to have the highest searched fractions for this parameter space for single surveys, factors of approximately 2 and 10 greater than the next highest, respectively. However, the highest

Table 1. MWA observing parameters

Parameter	Value
Central frequency	113.28 MHz
Total bandwidth	30.72 MHz
Number of imaged channels	2 400
Channel separation	10 kHz
Synthesised beam FWHM	$1.0'$
Primary beam FWHM	$30°$
Phase centre of image (J2000)	08h35m27s–45d12m19s
Total integration time	17 h

FWHM = Full Width at Half Maximum

search fractions still sit at an order of 10^{-18}, indicating that only a vanishingly small fraction of the SETI parameter space has been covered thus far.

While this conclusion may appear discouraging, cause for encouragement comes from the fact that SETI surveys can increasingly be performed effectively as commensal science in parallel with primary astrophysical investigations. This has been our approach using the MWA, whereby we utilise data collected and processed in wide field searches for low-frequency spectral lines (e.g. Tremblay et al. 2018). The *FAST* collaboration intends to complete commensal and dedicated SETI experiments, using a real-time data processing pipeline originally developed for the *SETI@Home* platform to search for technosignatures from 1 to 1.5 GHz during normal science operations (Zhang et al. 2020; Li et al. 2020). Similar ideas exist for commensal searches being planned with MeerKAT (Gajjar et al. 2019).

We continue this approach with the MWA here, adding a survey field centred on the Vela Supernova Remnant. In Section 2, we describe the observations and data processing, including increments in the quality of the data processing that lead to almost an order of magnitude improvement in our flux density sensitivity with commensurate improvements in our EIRP detection limits (for a fixed distance). In Section 3, we describe our results, examining the six known exoplanets in the Vela field as well as the full population of stellar systems in the field (millions of systems). In Section 4, we discuss our results and conclusions.

2. Observations and data processing

The MWA (Tingay et al. 2013) is a low-frequency interferometer operating between 70 and 300 MHz at the MRO in Western Australia. In 2018, the telescope was upgraded to the 'Phase II' array (Wayth et al. 2018), doubling the number of aperture array tiles from 128 to 256 and approximately doubling the maximum baseline from 3 to 5.5 km.

Observations of the Vela region took place between 2018 January 5 and 2018 January 23 for a total of 30 h, the details of which are summarised in Table 1. These observations were taken during the building and commissioning of the Phase II array and included 91 of the new 128 tiles. Of the 30 h of observation, 17 h were free from imaging artefacts likely caused due to the instrument being actively worked on during the day, while the observations were taken at night.

The MWA has an instantaneous bandwidth of 30.72 MHz that is distributed between 3072×10 kHz fine frequency channels. Our data were processed following the procedure detailed in Tremblay et al. (2017) and Tremblay (2018) but a summary is provided here and in Figure 1. The bandpass and phase solutions were derived

each night from a 2-min observation of Hydra A (a LINER galaxy with a flux density of 243 Jy at 160 MHz Kühr et al. 1981). The solutions were further refined by using self-calibration before they were applied to each 5-min observation of the Vela region field.

For each of the 5-min observations, the fine frequency channels (10 kHz) are imaged at a rate of 100 fine channels per every 1.28 MHz coarse channel to avoid channels affected by aliasing. This means only 78% of the band is imaged. The Phase II configuration of the MWA used in these observations removed the compact core and had shortest baselines of 1.5 km. In order to obtain as much sensitivity to diffuse emission as possible, all images were created using a Briggs weighting of 0.5. This produced a field-of-view of 400 deg^2 and a synthesised beamwidth of $1'$.

In previous SETI surveys completed with the MWA towards the Galactic Centre and the Orion Molecular Cloud, only 4 and 3 h, respectively, of observations were obtained. In this survey, 17 h of total integration time is used to provide our deepest low-frequency survey, producing a mean spectral RMS (root mean squared) of 0.05 Jy beam^{-1} across much of the field, in comparison to the previous 0.35 Jy beam^{-1} RMS.

The MWA is situated in an RFI-protected environment but occasional intermittent interference occurs (Offringa et al. 2015; Sokolowski, Wayth, & Ellement 2017). Each 5-min observation was flagged using AOFLAGGER (Offringa et al. 2015) to remove strong sources of radio frequency interference (RFI) signals from the raw visibilities based on statistical methods. This is not expected to impact our science goals, as the chance of a real astronomical or signal from an ETI being strong enough to be flagged in a single 5-min observation is very small. It is estimated that this process removes less than 5–20% of the total visibilities, having little impact on an observation's sensitivity. For these observations, after integrating each of the snapshot images, significant narrow-band RFI was detected in the commercial FM radio bands between 98 and 108 MHz. This left 64% of the band available for narrow-band signal searches.

These data are commensally searched for spectral line signals of an astrophysical nature, which will be reported in a separate publication (Tremblay et al. ApJ Submitted). An example of a typical spectrum with no significant signal, as seen towards HD 75289 b, is shown in Figure 2.

The source finding software AEGEAN (Hancock, Trott, & Hurley-Walker 2018) is used to search each of the 2 400 (10 kHz) fine frequency channels independently for signals over a 5σ limit. AEGEAN works by fitting Gaussians to the pixel data and applies a correction for the background[a] to calculate the flux density for potential sources. Any potential source is further evaluated based on various quality control checks, including but not limited to, ensuring the signal is greater than 5σ in both the spectral and image plane. Any remaining signals are cross-referenced to a combination of chemical databases and new chemical modelling reported in a future publication. Following this search, we found no signals of an unknown nature.

3. Results

Utilising the processed data described in Section 2, we have access to the spectrum across our bandwidth at 10 kHz resolution, for every pixel in our 400 deg^2 field-of-view. Thus, as per our previous work (Tingay et al. 2018; 2016), we can examine the spectrum at

---

[a]The background is defined by the 50th percentile of flux distribution in a zone 30 times the size of the synthesised beam.
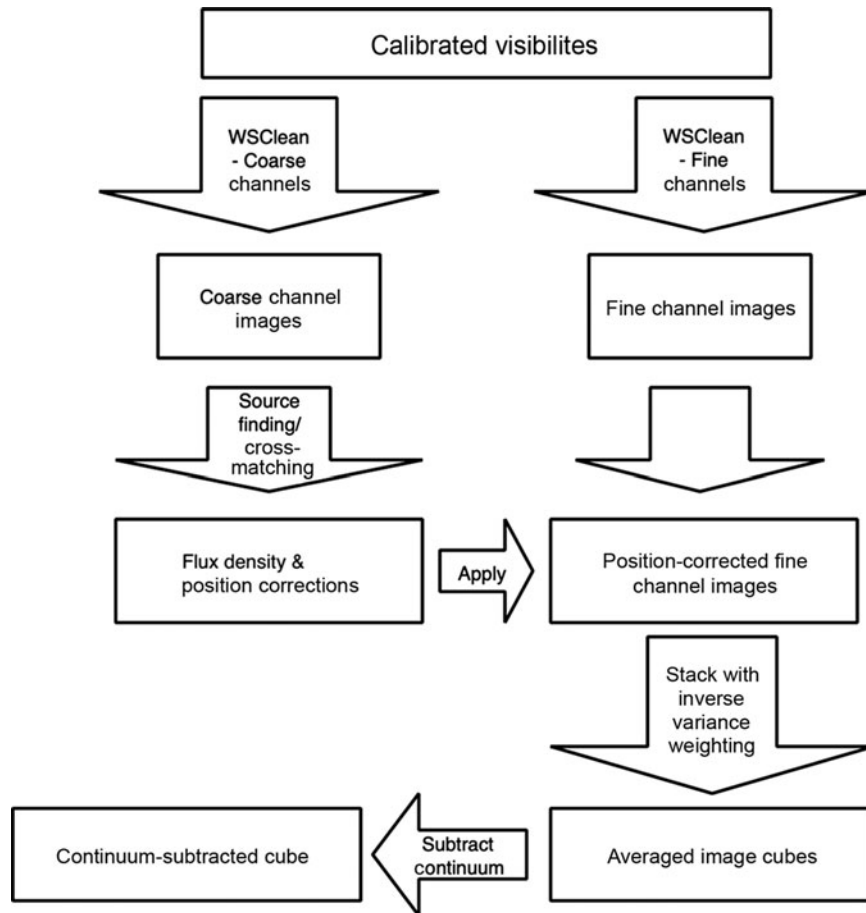
Figure 1. Summary of the data processing pipeline from Figure 2 of Tremblay et al. (2017) used to create integrated spectral cubes with the MWA.

the locations of stellar systems with known exoplanets and search for narrow-band signals that may constitute technosignatures. We undertake this examination below in Section 3.1. Further, given that only a tiny fraction of the exoplanets in this field are known, we can also undertake a blind survey of all stellar systems in the field with known distances from *Gaia* (Bailer-Jones et al. 2018) and undertake the same search. We undertake this examination in Section 3.2, below.

To calculate the upper limit on the total EIRP, we use the equation:

$$\text{EIRP(W)} < 1.12 \times 10^{12} S_{\text{rms}} R^2, \tag{1}$$

where S_{rms} is the RMS intensity value in Jy beam^{-1} and R is the distance to the stellar system in pc. This assumes that the transmission bandwidth is matched to the MWA fine channel bandwidth of 10 kHz. For transmission bandwidths less than 10 kHz, the maximum EIRP estimates are increased by $\frac{10kHz}{\Delta\nu_t}$, where $\Delta\nu_t$ is the transmission bandwidth. For example, a 10-Hz transmission bandwidth would cause our EIRP upper limits to be raised by a factor of 1000.

3.1. Known exoplanets in the survey field

A search of our field-of-view in the Exosolar Planets Encyclopedia Catalog[b] (as of March 2020) returns six exoplanets hosted by five

[b] http://exoplanet.eu/catalog.

stellar systems. These exoplanets are listed in Table 2, including basic parameters of the exoplanets, their stellar host, and the radio observations. In no case were any narrow-band signals detected towards these objects in our observing band at or above a level of 5σ. As in our previous work, we assign upper limits to the EIRP based on the RMS of the measured spectrum, listed in Table 2.

3.2. Other stellar systems in the survey field

Given the small number of known exoplanets associated with the stellar systems in this field, it is likely that a vast number of exoplanets remain unknown. Thus, we examine the general limits we can derive for stars in this field. We do this by examining the *Gaia* catalogue, extracting the distances of stars within the field determined by their parallax measurements (Bailer-Jones et al. 2018). There are 10 355 066 such stars within the field-of-view for this survey. As no detections were made in the search discussed in Section 2, we utilise the RMS value as a function of position across our field and the coordinates and distances of the stars, to derive the EIRP upper limit histogram for all 10 355 066 stars with a distance smaller than 6 350 pc in Figure 3. As the distribution of distances is dominated by stars within the spiral arm of the Galaxy at 1.5–2.5 kpc, the EIRP upper limits are also very large, orders of magnitude larger than the lowest upper limits from our previous work.

**Table 2.** Known exoplanets in the survey field, from the exoplanet catalogue: http://exoplanet.eu/

Designation	RA (J2000) hh:mm:ss	Dec (J2000) dd:mm:ss	Distance (pc)	MSin(i) (M_J^a)	Period (days)	Spectral type[b]	Detection method[c]	RMS (Jy beam^{-1})	EIRP[d] (10^{13} W)
HD 75289 b	08:47:40.0	−41:44:12	28.94	0.47	3.50928 $\pm 7.2946 \times 10^{-5}$	G0 V	RV	0.034	<3.2
HD 73526 b	08:37:16.0	−41:19:08	99.0	2.25 ± 0.12	188.9 ± 0.1	G6 V	RV	0.048	<53
HD 73526 c	08:37:16.0	−41:19:08	99.0	2.25 ± 0.13	379.1 ± 0.5	G6 V	RV	0.048	<53
HD 70642 b	08:21:28.0	−39:42:19	28.8	2.0	2231 ± 400	G5 IV-V	RV	0.039	<3.7
DE0823-49 b	08:23:03.0	−48:47:59	20.69 ± 0.06	−	247.75 ± 0.64	−	I	0.044	<2.1
KELT-15 b	07:49:40.0	−52:07:14	201.0 ± 19	0.91 ± 0.22	3.329441 $\pm 1.6 \times 10^{-5}$	−	PT	0.052	<237

[a] Mass of planet times the sine of orbit inclination, in Jupiter masses.
[b] Spectral type of host star.
[c] RV = radial velocity; I = imaging; PT = primary transit.
[d] Equivalent Isotropic Radiated Power.
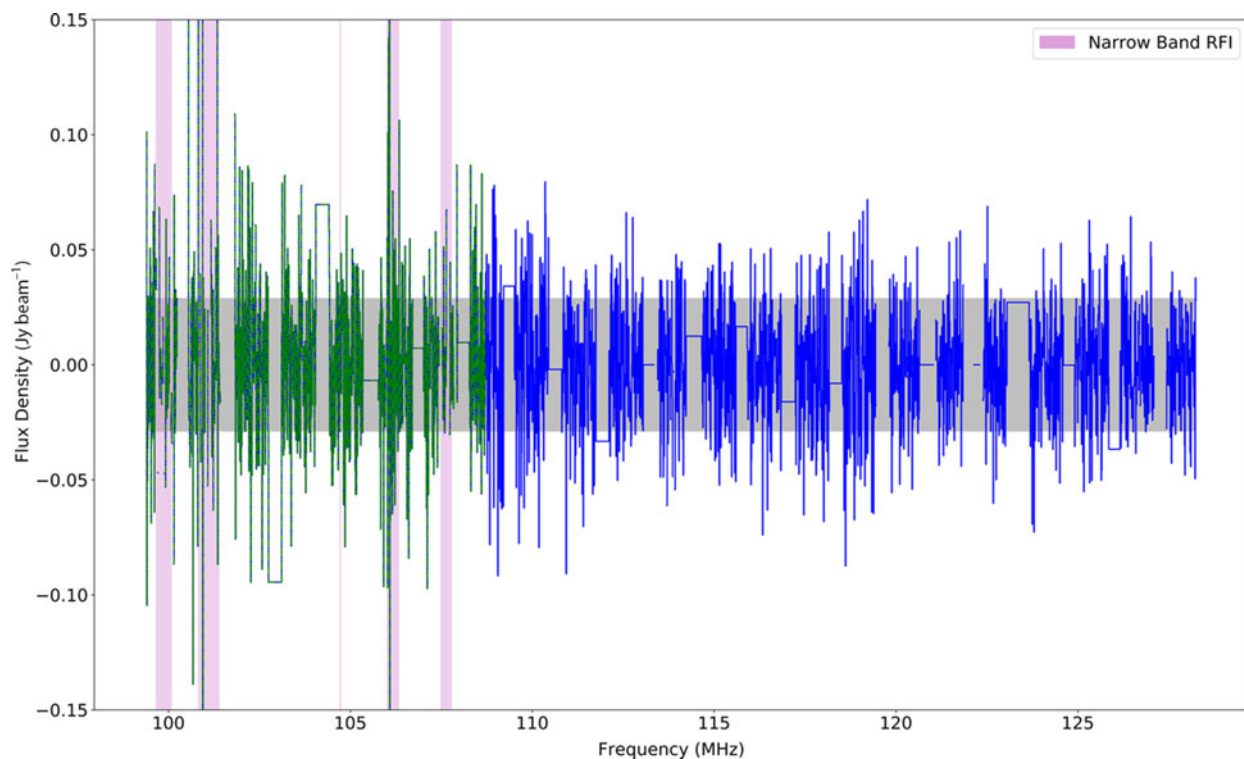
Figure 2. MWA spectrum for a data cube, with a total integration time of 17 h, used within this survey at the position of HD 75289 b. Some of the channels in the lower end of the band are affected by narrow-band RFI. The vertical shaded areas mark regions of known narrow-band RFI and the green region of the spectrum shows the top end of the FM band. Flagged channels are blanked out in the spectrum. The horizontal grey shaded region represents the $\pm 1\sigma$ RMS value used in Table 2.

To examine the most interesting part of this distribution, at low values of EIRP upper limit, we show the EIRP upper limit histogram for those stars within 30 and 50 pc in Figure 4. For the 10 closest stars, Table 3 lists the RMS and derived EIRP limits in more detail (excluding those systems referenced in Table 2).

4. Discussion and conclusion

The median distance for the six known exoplanet systems in the Vela field is 28.8 pc (treating HD 73526 b and c as a single system), compared to 50 pc for the 22 exoplanets examined by Tingay et al.

(2018) and ≈2 kpc for the 45 exoplanets examined by Tingay et al. (2016). Coupled with the sensitivity improvements we obtained (gained from the increased integration time of 17 h compared to the previous 4 h) described in Section 2, the median EIRP upper limit from this work is therefore an order of magnitude better than the median upper limit from Tingay et al. (2018). This represents continued improvement in our techniques and general upper limits. Our best upper limit from Table 3 of 6.2×10^{12} W (not for a known exoplanet) approaches a 50% improvement on our best upper limit from Tingay et al. (2018), still noting that an EIRP of 10^{12} W is high compared to the highest power transmitters on Earth at these frequencies (see Tingay et al. 2016 for a discussion).

Table 3. *Gaia* stellar systems in the survey field, from the *Gaia* DR2 release.

Designation	RA (J2000) hh:mm:ss	Dec (J2000) dd:mm:ss	Est. distance (pc)	RMS (Jy beam^{-1})	EIRP[a] 10^{13} (W)
5534076974490020000	08:00:39.6	−41:09:59.16	10.58 ± 0.26	0.058	<0.774
5528866839863560000	08:43:17.6	−38:52:51.30	11.18 ± 0.00	0.044	<0.620
5521313740446190000	08:15:13.0	−42:45:40.83	12.60 ± 0.27	0.039	<0.733
5522879208777730000	08:27:11.5	−44:59:13.17	13.76 ± 0.01	0.033	<0.698
5329084752471810000	08:44:38.3	−48:05:08.67	14.56 ± 0.01	0.035	<0.845
5329751125239010000	08:43:10.5	−46:59:28.18	15.55 ± 0.02	0.042	<1.14
5529120822749720000	08:40:40.8	−38:32:38.49	16.04 ± 0.02	0.036	<1.06
5328649002269670000	08:53:15.0	−48:12:49.59	16.17 ± 0.31	0.054	<1.66
5329580357345450000	08:47:19.1	−46:52:49.80	16.47 ± 0.01	0.048	<1.47
5514929155583860000	08:23:02.8	−49:12:01.08	20.66 ± 0.20	0.042	<2.08

[a]Equivalent Isotropic Radiated Power.
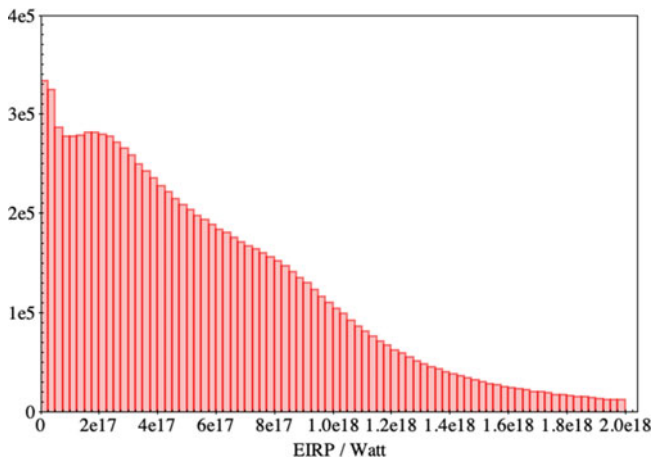
Figure 3. Histogram of EIRP upper limits based on the distribution of stellar distances (set to a maximum of 6350 pc) from the *Gaia* catalogue.
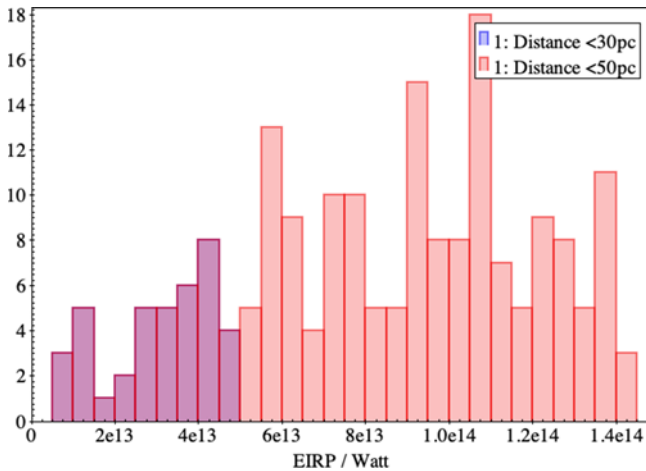
Figure 4. Histogram of EIRP upper limits based on the distribution of distances from the *Gaia* catalogue, with a focus on sources with distances <50 and <30 pc.

Sheikh et al. (2020) recently completed an in-depth analysis of 20 stars within the Earth transit zone between 3.95–8 GHz with the NRAO Green Bank Telescope (GBT). They determined an EIRP of detectable narrow-band signals that ranged from 47 to 17590×10^9 W for stellar distances between 7 and 143 pc. These are similar distances to the stars we present in Table 3 for the nearby stars from *Gaia* in the Vela field, but our sample represents a much larger population of on-average closer sources. Sheikh et al. (2020) also convert their EIRP values to the fraction of signal capacity for the Aricebo Transmitter (L_A). Their value of 0.033 for a star at 27 pc is a factor of two lower than for a star in our survey at the same distance (0.068), recognising the difference in frequency between the GBT and the MWA and the fact that the GBT has better frequency resolution than the MWA.

For the first time, we obtain simultaneous upper limits on EIRP for in excess of 10 million stellar systems without known exoplanets, although the EIRP limits for the majority of distant systems are well above 10^{13} W. For any future exoplanet discoveries for systems in this field, the low-frequency EIRP upper limits are immediately available from our data.

Seto & Kashiyama (2020) completed an astrometric study of F-,G-, and K-type stars in *Gaia* Data Release 2 for interstellar communications, from the view point of the sender, and concluded that surveys like *Gaia* will be necessary to target these potential signals. Petigura, Marcy, & Howard (2013) suggest that approximately 20% of Galactic Sun-like stars could have Earth-sized planets in their habitable zones and Kipping (2020) suggests that searching for technosignatures from stars with stellar types much earlier than our Sun may not be necessary, as life is unlikely to ever evolve. This means that matching SETI survey data to the *Gaia* survey is going to be an important approach for the future of SETI.

We compare our results to Figure 5 of Price et al. (2020), in which the results of previous surveys are presented in a plane defined by minimum EIRP (EIRP$_{min}$) at the maximum stellar distance and Transmitter Rate, $(N_{star}(\frac{\nu_c}{\nu_{tot}}))^{-1}$, where N_{star} is the total number of stars searched and ν_c and ν_{tot} are the central frequency of the band (113.28 MHz) and the total bandwidth (30.72 MHz), respectively. For our survey using the *Gaia* catalogue, we see that our results sit below the most constraining limits set by prior work within this particular parameter space when using a distance of 1.7 kpc and a channel bandwidth of 10 kHz.

We also consider a different metric, utilising the method of Wright et al. (2018) in order to calculate the 'haystack fraction' accessible to our observations of the Vela region. This metric takes into account the observational parameters without significant
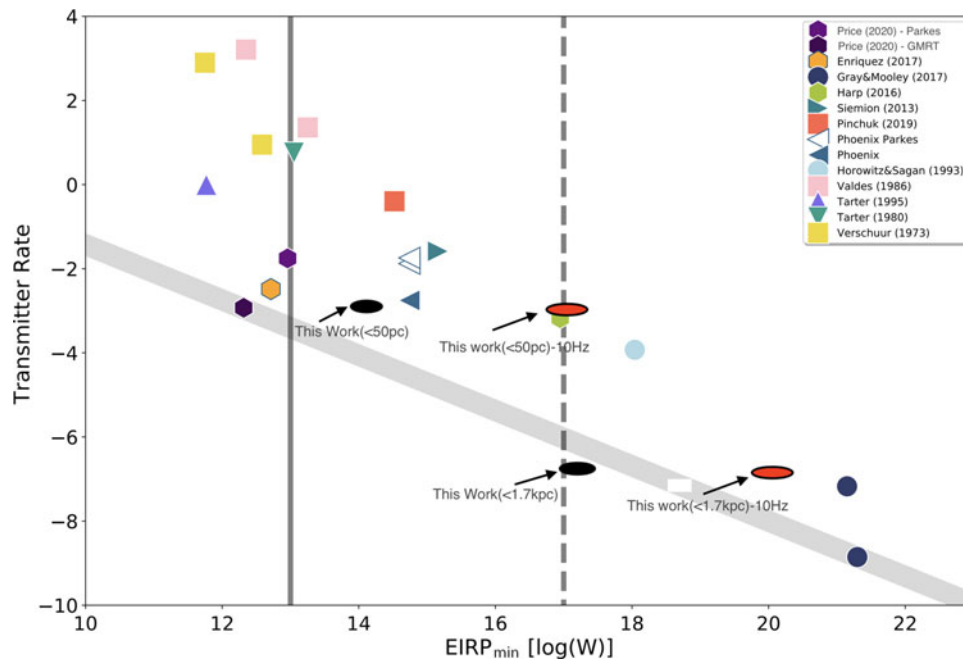
Figure 5. Figure 5 from Price et al. (2020) with our results for the *Gaia* catalogue survey (Section 3.2) shown for comparison. We report the results using a maximum RMS of 0.06 Jy beam^{-1} and when we limit the distances to less than 50 pc, as per Figure 4 and for all stars less than 1.7 kpc. The value of 1.7 kpc is chosen as it is the distance to the Vela Molecular Cloud complex, a stellar-rich environment towards the Carina-Sagittarius spiral arm. The black ovals are the EIRP values per Equation (1) assuming a 10-kHz channel bandwidth and the red ovals are using the EIRP values assuming a transmission bandwidth of 10 Hz. These results span the diagonal grey line representing a fit between the previous most constraining data points for Transmitter Rate and EIRP$_{min}$ at the most distant star when using the MWA channel bandwidth. The solid and dashed vertical lines represent the EIRP of the Arecibo planetary radar, and the total power from the Sun incident on the Earth, respectively.

assumptions. We find the haystack fraction to be $\sim 2 \times 10^{-16}$, which is almost two orders of magnitude higher than the highest previous fraction listed in Wright et al. (2018), which was for our previous observations of the Orion Molecular Cloud (Galactic Anticentre) field. Our new result yields the haystack fraction almost three orders of magnitude higher than the largest non-MWA survey listed by Wright et al. (2018).

Recently, Westby & Conselice (2020) described the so-called Strong Astrobiological Copernican scenario, in which life must arise in a system on timescales comparable to those experienced on Earth (4.5–5 Gyr) and posit on this basis that at least $36 \pm^{175}_{32}$ civilisations capable of generating technosignatures exist in our Galaxy. The closest system to Earth would be $17\,000 \pm^{33\,600}_{10\,000}$ lt-yr distant. The numbers are not large and represent a very small part of the haystack fraction parameter space, throwing into focus that SETI experiments will need to enter the statistical domain of *Gaia*-sized samples.

Overall, our MWA surveys show the rapid progress that can currently be made in SETI at radio frequencies, using wide field and sensitive facilities, but also show that SETI surveys have a long way to go. The continued use of the MWA, and the future similar use of the SKA at much higher sensitivities, offers a mechanism to make significant cuts into the haystack fraction of Wright et al. (2018), while maintaining a primary focus on astrophysical investigations, making excellent commensal use of these large-scale facilities.

4.1. Facilities

This scientific work makes use of the MRO, operated by CSIRO. We acknowledge the Wajarri Yamatji people as the traditional

4.2. Computer services

4.3. Software

The following softwares were used in the creation of the data cubes:

- AOFLAGGER and COTTER—Offringa et al. (2015)
- WSCLEAN—Offringa et al. (2014); Offringa & Smirnov (2017)
- AEGEAN—Hancock et al. (2018)
- MIRIAD—Sault, Teuben, & Wright (1995)
- TOPCAT—Taylor (2005)

References

Bailer-Jones, C. A. L., Rybizki, J., Fouesneau, M., Mantelet, G., & Andrae, R. 2018, AJ, 156, 58

Gajjar, V., et al. 2019, in BAAS, 223 (arXiv:1907.05519)

Gray, R. H., & Mooley K., 2017, AJ, 153, 110

Hancock, P. J., Trott, C. M., & Hurley-Walker, N. 2018, PASA, 35, e011

Kipping, D. 2020, in American Astronomical Society Meeting Abstracts, 454.03

Kühr, H., Witzel, A., Pauliny-Toth, I. I. K., & Nauber, U. 1981, A&AS, 45, 367

Li, D., Gajjar, V., Wang, P., Siemion, A., Zhang, Z., & FAST Collaboration 2020, arXiv e-prints, p.arXiv:2003.09639

Offringa, A. R., & Smirnov, O. 2017, MNRAS, 471, 301

Offringa, A. R., et al. 2014, MNRAS, 444, 606

Offringa, A. R., et al. 2015, PASA, 32, e008

Petigura, E., Marcy, G. W., & Howard, A. 2013, in American Astronomical Society Meeting Abstracts #221, 216.05

Price, D. C., et al. 2020, AJ, 159, 86

Sault, R. J., Teuben, P. J., & Wright, M. C. H. 1995, in Astronomical Society of the Pacific Conference Series, Vool. 77, Astronomical Data Analysis Software and Systems IV, ed. R. A. Shaw, H. E. Payne, & J. J. E. Hayes, 433 (arXiv:astro-ph/0612759)

Seto, N., & Kashiyama, K. 2020, arXiv e-prints, p.arXiv:2003.03511

Sheikh, S. Z., Siemion, A., Enriquez, J. E., Price, D. C., Isaacson, H., Lebofsky, M., Gajjar, V., & Kalas, P. 2020, arXiv e-prints, p.arXiv:2002.06162

Sokolowski, M., Wayth, R. B., & Ellement, T. 2017, in Radio Frequency Interference (RFI), 7833541, doi:10.1109/RFINT.2016.7833541

Taylor, M. B. 2005, in Astronomical Society of the Pacific Conference Series, Vol. 347, Astronomical Data Analysis Software and Systems XIV, ed. P. Shopbell, M. Britton, & R. Ebert, 29

Tingay, S. J., et al. 2013, PASA, 30, e007

Tingay, S. J., Tremblay, C., Walsh, A., & Urquhart, R. 2016, ApJ, 827, L22

Tingay, S. J., Tremblay, C. D., & Croft, S. 2018, ApJ, 856, 31

Tremblay, C., 2018, PhD thesis, Curtin University

Tremblay, C. D., et al. 2017, MNRAS, 471, 4144

Tremblay, C. D., Jones, P. A., Cunningham, M., Hurley-Walker, N., Jordan, C. H., & Tingay, S. J. 2018, ApJ, 860, 145

Wayth, R. B., et al. 2018, PASA, 35, 33

Westby, T., & Conselice, C. J. 2020, ApJ, 896, 58

Wright, J. T., Kanodia, S., & Lubar, E. 2018, AJ, 156, 260

Zhang, Z.-S., et al. 2020, ApJ, 891, 174